JEAS

Journal of Engineering and Applied Sciences 5 (2010)

JOURNAL OF ENGINEERING AND

Electrical machines modelling using a circuit – coupled finite element method

A. W. Nwosu, [1]H. N. Ude and [2]S. S. N. Okeke

Department of Electrical/Electronic Engineering Anambra State University Uli
[1]Raw Materials Research and Development Council, Abuja.
[2]Department of Electronic and Computer Engineering Nnamdi Azikiwe University Awka

Abstract

A non-linear circuit – coupled two dimensional (2D) finite element model for use in the dynamic simulation of electrical machines with multiple sets of windings, connected to an external electrical circuit, and with rotating parts was presented in this paper. An inductance is introduced to account for the 3D end effects on phase inductance, due to the end windings and axial fringing field. The model is applied to the simulation of two types of electrical machines, a permanent magnet generator and a switched reluctance motor. The modeling procedures are described and simulation results are presented. The calculated performances are compared with test results to validate the modeling.

Keywords: Electrical machines, switched reluctance motor, permanent magnet generator, inductance.

Introduction

Electrical machines are rotary or linear moving power devices with multiple sets of coils connected to an external electrical circuit. Two examples for the modern types of electrical machines are a permanent magnet generator (PMG) and a switched reluctance motor (SRM). The PMG studied has a radial-flux, outer-rotor, slotted-stator and surface-mounted magnet topology [1], as shown in Figure 1(a). The permanent magnets are bonded to the inner surface of a steel drum that rotates around a stationary stator with conventional three-phase windings. The SRM to be analyzed has teeth on both the stator and the rotor, but only the stator carries windings [as shown in Fig. 1(b).

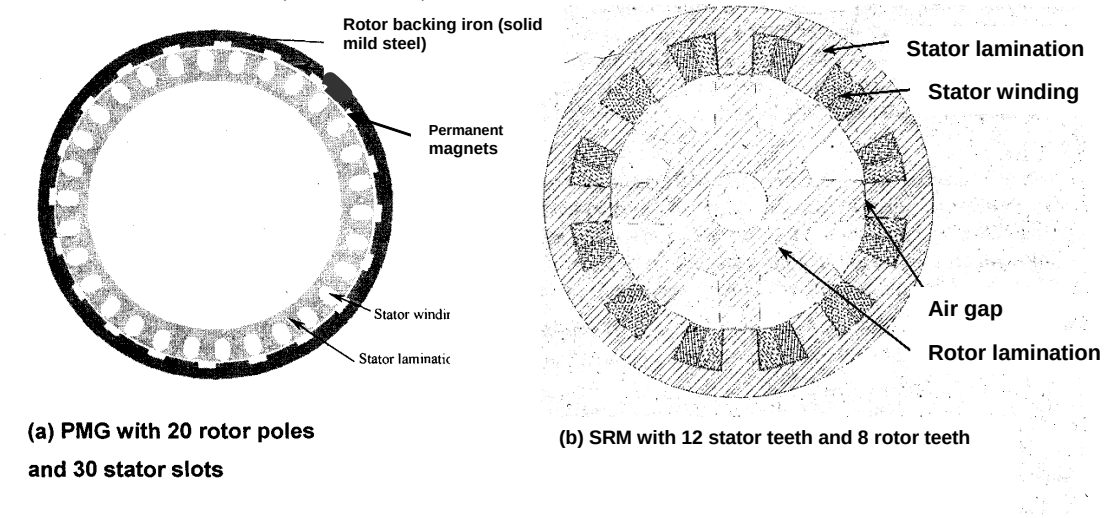

Figure 1. Sketch of two electrical machines

In dynamic simulations, the electrical circuit and magnetic circuit of electrical machines are usually separated. The electrical parameters, such as no-load phase emf and phase inductance of the PMG, or static characteristics of flux linkage versus rotor position and current of the SRM, are obtained numerically or experimentally. The no-load phase emf or nonlinear magnetization data are tabled or fitted with an analytical equation. The system is then simulated by a computer program or a standard modeling package, such as Spice [3-4] Saber [5] and Simulink [6]. The traditional methods usually ignore the effect of the multi-phase currents on the saturation, and its accuracy depends on the fitting of the static magnetization data.

With recent developments in numerical modeling, a circuit-coupled 3D finite element method (FEM) has been used for simulations of electrical machines [7]. However, 3D FEM is computationally expensive and time consuming for the design optimization of electrical machines. 2D FEM coupled to external circuits by using Ansoft Maxwell EMSS has been reported in [8]. Ansoft Simplorer coupled with Magsoft Flux2D was used for the study of a mutually coupled SRM [9], in which 3D end effects were ignored.

This paper presents a nonlinear analysis of electrical machines based on ANSYS circuit-coupled 2D FEM including 3D corrections, which is applied to the two types of electrical machines shown in Figure 1. The modeling procedures of the circuit-coupled 2D FEM re described. To account for the 3D end effects on phase inductance due to the end windings and the axial fringing field, an inductance is introduced in the 2D analysis. For the PMG, simulation results are presented for a rectifier load and compared with experiments and calculation from equivalent circuit methods. The simulations of the SRM for various load conditions at different speeds are performed to find the optimal turn-on and turn-off angles, and compared with test results.

Procedure

Permanent Magnet Generator

For a PMG with an integer number of slots per phase per pole pair, only two poles of the PMG needs to be studied, as the machine is even-periodically symmetrical for two poles.

The meshes for the stator and rotor were generated separately. A half slot pitch of the stator with half the air gap was meshed and mirrored to form one slot, and then copied to form two pole pitches. The same approach was applied to the rotor meshes. The rotor with half air gap meshes was rotated by the specified rotor position angle and joined to the stator mesh along the inner side of the half air gap by using coupling equations. One requirement of this method is to mesh the common side of the half air gap attached to the stator and rotor with the same number of divisions. The mirrored meshes for each stator slot and each rotor pole eliminate numerical errors due to an asymmetric mesh. The joining of the stator and rotor meshes by using coupling equations maintains the same number of nodes for the model whenever the rotor rotates, which is essential for the transient analysis.

Figure 2(a) shows the magnetic finite element meshes for a specified rotor position. The nodes on the two radial edges of the stator and rotor are coupled by even periodic boundary conditions using the PERBC2D command. The surrounding air inside and outside the PMG was modelled to a distance of 5 times the air gap radially. On the inner edge of the air inside the stator and on the outer edge of the air outside the rotor the flux is assumed to be parallel to these edges (i.e. no flux escapes out of the surrounding air).

The stator lamination and rotor iron (solid mild steel) are represented by their single-valued non-linear B-H characteristics. The stator lamination can be modeled as a homogenous material along the axial direction, so its B-H characteristic can be corrected by using

$$B_{new} = I_{sf} \cdot B_{old} + (1 - I_{sf}) \cdot \mu_0 H \quad (1)$$

where I_{sf} is the lamination stacking factor. B_{old} and H are obtained from the manufacturer's data sheet. B_{new} is the corrected flux density corresponding to field strength, H.

The permanent magnet utilised has a square hysteretic loop. Because the induction curve for this material is linear, it can be simply approximated as a fixed permeability of μ in all directions and a remanence of B_r in the magnetised direction. However, the remanence is temperature dependent, and is given by

$$B_r = B_{r20} \cdot (1 - \alpha_{br} \cdot (T - 20)) \quad (2)$$

where B_{r20} is the remanence at 20°C and α_{br} the temperature coefficient. T is the operating temperature of the magnet, which is equal to the ambient temperature plus the rotor temperature rise.

The elements in the magnet region are assigned to a local element coordinate system, whose X-axis is aligned with the rotor position. When the rotor rotates, the

magnetization direction of the magnets will be rotating as well.

The winding is magnetically modelled as air. The regions of the air gap, stator lamination, rotor mild steel, and permanent magnets are modeled with the PLANE element. If the resistivity of the rotor mild steel and permanent magnets are specified and PLANE 13 with VOLT and AZ degrees of freedom (KEYOPT(1)=6) is used for these two regions, eddy currents in the rotor mild steel and magnets can be calculated. For calculating the eddy currents, the mesh size for the region of interest should be less than their skin depth. Further discussion about the mesh size and calculation of eddy current losses in the rotor mild steel and magnets can be found in [1]

The region of the stator slots containing the stator winding is modelled using PLANE53 with the stranded coil option (KEYOPT(1)=3). The two halves of the phase winding are coupled to the two N3 in the external electrical circuit as shown in Figure 2(b).

The circuit is created by using CIRCUI24 and C1RCU elements. In the circuit, *L4* represents a difference in inductance between the 2D and 3D analyses, and accounts for the 3D end effects on phase inductance due to the end windings and the axial fringing field. *L4* can be calculated from static 2D and 3D FEMs or an empirical formula. R20 is an equivalent resistor to account for the no-load iron loss in the stator lamination. The loss resistor should be paralleled with the phase emf. To implement this, the resistivity of the coil region is set to a very small value ($10^{-12}\Omega$m in the model) and the phase resistance is represented by *R5* in the circuit. The full-wave diode rectifier is represented by the diode element *D6-D8*. The load can be a resistor or a battery. In the figure, *R9* and *C10* represent the load resistor and capacitor respectively.

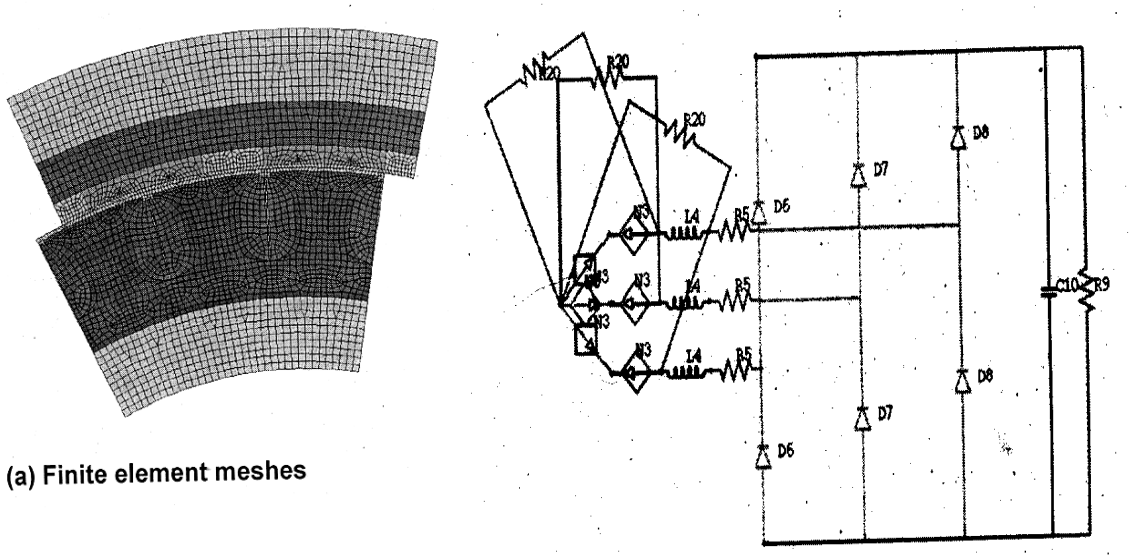

(a) Finite element meshes

(b) Electrical circuit

Figure 2: Circuit-coupled FEM model of the PMG

Switched Reluctance Motor

For the conventional m-phase *Ns/Nr* SRM (where the number of stator teeth *Ns=Nx2m*, the number of rotor teeth *Nr=Nx2* (m-1), and N is an integer number), only a region of m stator tooth pitches and (m-1) rotor tooth pitches need to be studied, as the motor is odd-periodically symmetrical for every m stator teeth under both single-phase and multi-phase excitation. For a SRM with 12 stator teeth and 8 rotor teeth, 3 stator teeth and 2 rotor teeth are modeled. Figure 3 shows the circuit-coupled 2D FEM model of the SRM for a specified rotor position. The meshes, material properties, and boundary conditions are similar to the PMG described above. The main difference between the PMG and SRM models is the electrical circuit.

By using CIRCU 124 and CIRCU125 elements, the circuit model shown in Figure 3(b) is an approximation of a 3-phase SRM connected to a DC link through a conventional six-switch converter operating under voltage control. The phase current, and hence the torque output of the SRM, is determined by the turn-on and turn-off angles of the phase voltage

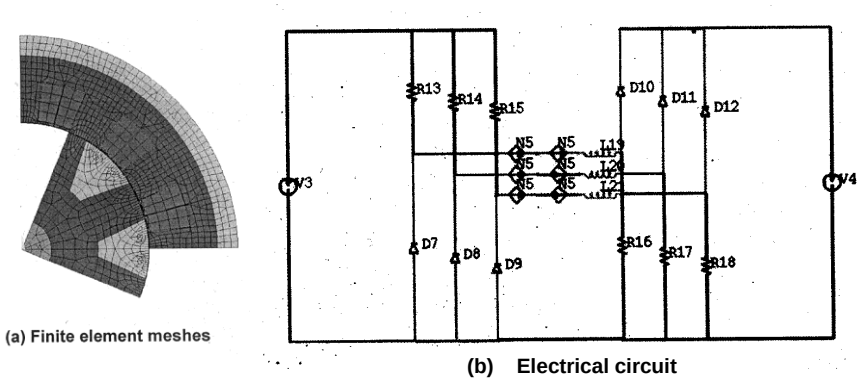

Figure 3. Circuit-coupled FEM model of the SRM

Two voltage sources are used to simulate the Permanent Magnet Generator (PMG) voltage control. The turn-on voltage, V3, is the PMG ratio multiplied by the DC link voltage, and the turn-off voltage, V4, is the inverted DC link voltage. The voltage applied to each phase is controlled, in accordance with the rotor positions, by its top and bottom transistors. The transistors are represented by resistors *R13-R18*. Resistance equals 10^{-6} Ω for the on-state and 10^{6} Ω for the off-state. V3 is reduced by 4.3 V to account for the on-state voltage drops of the top and bottom transistors. The free-wheel diodes (forward voltage drop I V) are represented by *D7-D12*. Two *N5* in each phase represents the two halves of the phase winding and are coupled to the finite element region of the stator coils in Figure 3(a). *L19-L21* represents an unsaturated difference inductance for each phase between the 2D and 3D analyses, and accounts for the 3D end effects on phase inductance due to the end windings and the axial fringing field. *L19-L21* can be calculated from static 2D and 3D FEMs when a small current is fed into one phase. Figure 4 shows the unsaturated phase inductance and difference inductance as a function of the rotor position.

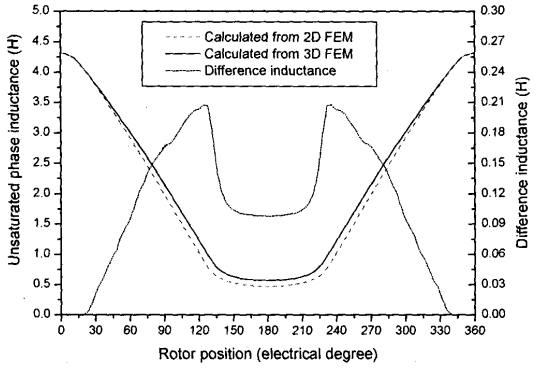

Figure 4. Inductance as a function of rotor position of the SRM

The iron losses of the stator and rotor laminations for the SRM studied were not included in the model since they are low. When the iron losses are high, they can be represented by variable resistors in parallel with the phase emfs as described in the circuit model of the PMG.

Analysis

For a given constant speed, an electrical cycle, i.e. 360^{0} (physically equals to the rotation of two pole pitches for the PMG and one rotor tooth pitch for the SRM), was divided into 120 discrete equidistant time steps. In each time step, the coupling equations joining the stator and rotor at the middle of the air gap were cleared. Then the rotor was rotated by 3° (electrical degree) using AGEN and re-joined to the stator by a set of new coupling equations.[7].

For the PMG, the magnetization direction of the rotor magnets was simultaneously changed by using EMODIF and LOCAL. For the SRM, the stator phase excitation and the phase difference inductance were simultaneously changed by modify the real constants of *R13-R18* and *L19-L21* in Figure 3(b). It is noted that this approach

gives reliable results, although changing element real constants between time steps is generally a non-standard use in ANSYS.

In the first time step, i.e. time is at 0 second (actually using 10^{-9} as ANSYS does not allow 0 as a time step), a static analysis was performed to establish the initial magnetic field. In the following time steps, the time integration effect was turned on by using TIMINT with ON option and ANTYPE with REST option. Consequently a transient analysis was restarted in each time step except the first time step, to include the time integration effect from the solutions in the previous time steps.

The magnetic and electrical parameters, such as torque, power, current and voltage, were calculated in each time step. When the phase currents and hence torque reach their stable values after a number of cycles, the average torque, power, and phase RMS currents in the last cycle were obtained. The friction torque of the PMG and SRM was ignored in the calculation. Only two electrical cycles need to be calculated for low speeds and about 10 cycles for high speeds.[10].

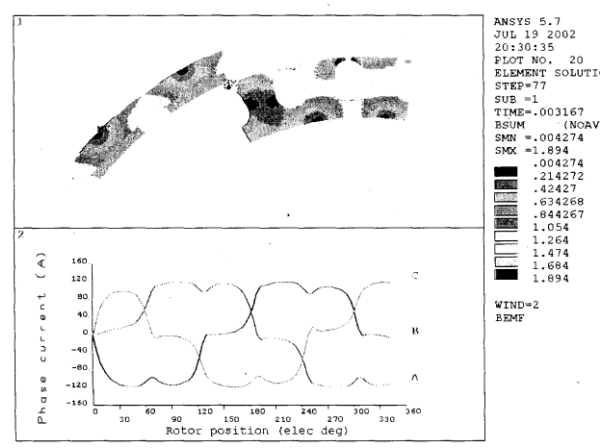

Figure 5. Simulation results for the PMG

Similarly, the simulation results for the SRM are shown in Figure 7. A comparison of the phase current between calculation and measurement for a specified load and speed is shown in Figure 8. There is a good agreement between the calculated and measured currents and torques.

For the SRM, the proposed circuit-coupled 2D FEM can be used to simulate single pulse operation, PWM voltage control and hysteresis current control. It can be used to evaluate control strategies of a SRM drive system, for example, finding the optimal turn-on and turn-off angles and PWM ratios, to achieve maximum efficiency for a given speed and torque. More detailed results have been reported in [10].

Analysis Results & Discussion

Figure 5 shows the simulation results of the PMG. The contour plot of flux densities in the stator lamination, rotor mild steel and magnets for the last time step is shown in window I. The currents in the stator phases versus the rotor position are given in window 2. For a specified load resistor, Figure 6 compares the calculated phase voltage and current with measurements. The predicted results from the equivalent circuit method are also shown in the figure. It can be seen that the circuit-coupled 2D FEM gives good agreement between calculated and measured results.

For the PMG, the proposed circuit-coupled 2D FEM can be used to calculate the performance for different load conditions, such as battery and resistor. The effects on the performance of the stator iron loss and eddy current losses in the rotor steel and magnets are included. This approach can also be applied to analyze the transient performance of the PMG when the windings are short circuited or speed variation occurs.

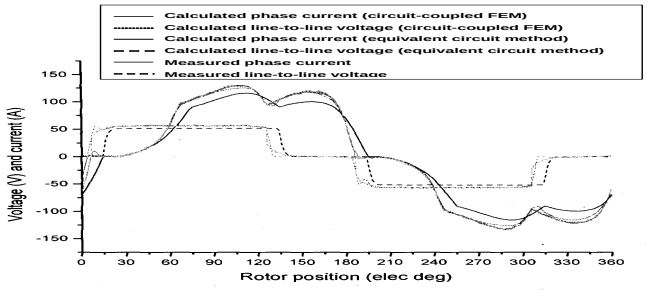

Figure 6. Comparison of calculated and measured results of the PMG

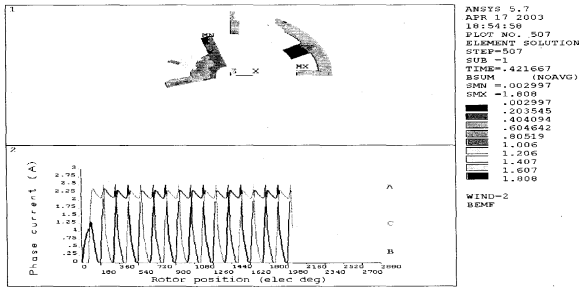

Figure 7. Simulation results for the SRM

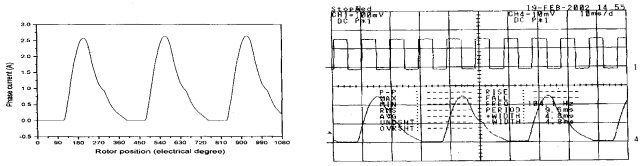

igure 8. Calculated (259 rpm, 12.6 Nm) and measured (259 rpm, 12 Nm, trace 4, 1A/div) hase current of the SRM

Conclusion

This paper has reported a nonlinear modeling method that involves circuit simulation and FEM simultaneously. In this modeling, the important effects of saturation and multi-phase excitation have been included. Although the finite element analysis is two dimensional, the 3D end effects on phase inductance due to the end windings and axial fringing field have been considered by introducing a variable difference inductance as a function of rotor position. The proposed method has been implemented in ANSYS and applied to the two types of electrical machines, PMG and SRM. The method has been validated by experimental results on the prototypes.

References

[1] W. Wu, J.B. Dunlop, S.J. Collocott, (2002) "Modelling of eddy-current losses in a surface-mounted NdFeB permanent-magnet generator," Proceedings of the Seventeenth International Workshop on *Rare-earth Magnets and Applications,* Newark, Delaware, USA, pp323-328.

[2] W. Wu, J.B. Dunlop, S.J. Collocott, and B.A. Kalan, (2003) "Design optimization of switched reluctance motor by electromagnetic and thermal finite element analysis, *"IEEE Transaction on Magnetics,* Vol. 39, No. 5.

[3] J. Faiz, J. Raddadi, and J.W. Finch, (2002), "Spice-based dynamic analysis of a switched reluctance motor with multiple teeth per stator pole," IEEE Transaction on Magnetics, Vol. 38, No. 4, pp 780-1788.

[4] 0. Ichinokura, S. Suyama, T. Watanabe, and, H.J. Guo, (2001), "A new calculation model of switched reluctance motor for use on Spice,*"IEEE Transaction on Magnetics,* Vol. 37, No. 4, pp2834-2836.

[5] S. Cao and K.J. Tseng, (2000), "Dynamic modeling of SRM including neighboring phase coupling effects," *Electric Machines and Power Systems,* Vol. 28, pp 141-1163.

[6] F.S. Soares and P.J. Costa Branco, (2001),"Simulation of a 6/4 switched reluctance motor based on Matlab/Simulink environment," *IEEE Transactions on Aerospace and Electronic Systems,* Vol. 37, No. 3.

[7] H.C. Lai, P.J. Leonard, D. Rodger, N. Allen, and P. Sangha, (1997), "3D finite element dynamic simulation of electrical machines coupled to external circuits," *IEEE Transactions on Magnetics,* Vol. 33, No.2.

[8] K.N. Srinivas and R. Arumugam, (2002), "Finite element analysis combined circuit simulation of dynamic performance of switched reluctance motors," *Electric Power Components and Systems,* Vol. 30.

[9] Y. Xu and D.A. Torrey, (2002)"Study of the mutually coupled switched reluctance machine using the finite element-circuit coupled method," *lEE Proc-Electr. Power Appl.,* Vol. 149, No. 2, pp8I-86.

[10] W. Wu, B.A. Kalan, H.C. Lovatt, (2003), "Time-stepping analysis of switched reluctance motor by coupling electrical circuit and electromagnetic finite element method," *Proceedings of the 6th International Conference on Electrical Machines and Systems,* Beijing, China, IEEE Catalogue 03EX782, International Academic Publishers, Beijing, pp728-731.

NOMENCLATURE:

2D	=	two Dimensional
3D	=	three Dimensional
PMG	=	permanent magnet generator
SRM	=	switched reluctance motor
FEM	=	finite element method
RMS	=	root means square
B	=	flux density
H	=	field strength
I_{st}	=	lamination stacking factor
B_{new}	=	corrected flux density
μ_r	=	fixed permeability
B_r	=	remanence
B_{r20}	=	remanence at 20^0C
T	=	operating temperature
D	=	diode

C	=	capacitor
R	=	resistor
N_s	=	number of stator teeth
N_r	=	number of rotor teeth
DC	=	direct current
N	=	phase winding
α_{bx}	=	the temperature coefficient